Stable isotope data as constraints on models for the origin of coralloid and massive speleothems: The interplay of substrate, water supply, degassing, and evaporation

Guglielmo A. Caddeo [a,*], L. Bruce Railsback [b], Jo De Waele [c], Franco Frau [a]

[a] Dipartimento di Scienze Chimiche e Geologiche, Università di Cagliari, Via Trentino 51, 09127 Cagliari, Italy
[b] Department of Geology, University of Georgia, Athens, GA 30602-2501, USA
[c] Dipartimento di Scienze Biologiche, Geologiche ed Ambientali, Università di Bologna, Via Zamboni 67, 40126 Bologna, Italy

ABSTRACT

Many speleothems can be assigned to one of two morphological groups: massive speleothems, which consist of compact bulks of material, and coralloids, which are domal to digitate in form. Faster growth on protrusions of the substrate occurs in the typical growth layers of coralloids (where those layers are termed "coralloid accretions"), but it is not observed in the typical layers of massive speleothems, which in contrast tend to smoothen the speleothem surface (and can therefore be defined as "smoothing accretions"). The different growth rates on different areas of the substrate are explainable by various mechanisms of $CaCO_3$ deposition (e.g., differential aerosol deposition, differential CO_2 and/or H_2O loss from a capillary film of solution, deposition in subaqueous environments). To identify the causes of formation of coralloids rather than massive speleothems, this article provides data about $\delta^{13}C$ and $\delta^{18}O$ at coeval points of both smoothing and coralloid accretions, examining the relationship between iso topic composition and the substrate morphology. In subaerial speleothems, data show enrichment in heavy isotopes both along the direction of water flow and toward the protrusions. The first effect is due to H_2O evaporation and CO_2 degassing during a gravity driven flow of water (gravity stage) and is observed in smoothing accretions; the second effect is due to evaporation and degassing during water movement by capillary action from recesses to prominences (capillary stage) and is observed in subaerial coralloids. Both effects coexist in smoothing accretions interspersed among coralloid ones (intermediate stage). Thus this study supports the origin of subaerial coralloids from domi nantly capillary water and disproves their origin by deposition of aerosol from the cave air. On the other hand, sub aqueous coralloids seem to form by a differential mass transfer from a still bulk of water toward different zones of the substrate along diffusion flux vectors of nutrients perpendicular to the iso depleted surfaces. Finally, this isotopic method has proved useful to investigate the controls on speleothem morphology and to obtain additional insights on the evolution of aqueous solutions inside caves.

1. Introduction

Speleothems are mineral deposits that are chemically precipitated in caves, and they include flowstones, stalactites, stalagmites, and many other less familiar but diverse forms (Hill and Forti, 1997). Most speleothems consist of sequences of layers readily recognizable in sections perpendicular to their growth surface. Petrographic observations of these sections reveal two specific types of the growth surface progres sion through time, leading to two very different morphologies of the resulting speleothem. To distinguish between these two specific patterns of growth and their relationship with time, this paper will distinguish between smoothing and coralloid accretions. The word

"accretion" refers to the material deposited in a single speleothem during a fixed period of time, which can be a continuous or discontinuous layer, because it is defined as a temporally bounded, rather than physically bounded, entity. "Smoothing accretion" will refer to an accre tion that is uniform or thinner on protrusions than in depressions of its substrate, tending to smooth any pre existing topography and to form a compact bulk of material (Fig. 1a). On the other hand, "coralloid accretion" will refer to an accretion that thickens gradually from the depressions toward the protrusions of the substrate and thus imparts domal to digitate forms to the resulting speleothem (Fig. 1b).

Sequences of coralloid accretions are usually defined as coralloids (Figs. 1, 2) or by the colloquial name "popcorn" (Hill and Forti, 1997). On the other hand, sequences consisting mostly of smoothing accretions have been designated as massive speleothems (Alonso Zarza et al., 2011) or bulk speleothems (White, 2012). These are further differenti ated into various types, depending on their location and general

* Corresponding author.
E-mail addresses: mesucosta@alice.it (G.A. Caddeo), rlsbk@gly.uga.edu (L.B. Railsback), jo.dewaele@unibo.it (J. De Waele), frauf@unica.it (F. Frau).
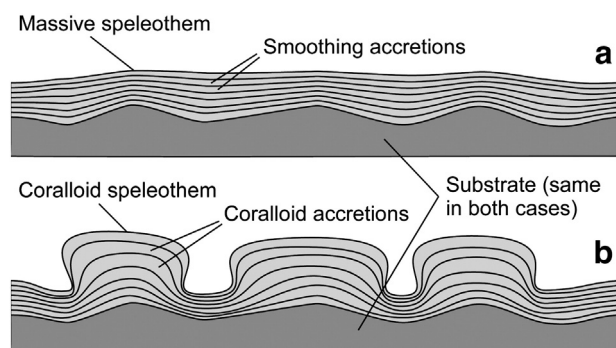
Fig. 1. Sketches illustrating a massive speleothem (a) and a speleothem consisting of coralloids (b). Both sketches show the accretions (material deposited in a single speleothem during a fixed period of time). Massive speleothems are sequences of typical smoothing accretions which do not grow faster on substrate protrusions than on substrate depressions (a). Coralloids are sequences of typical coralloid accretions growing faster on substrate protrusions than on substrate depressions (b).

morphology (e.g., flowstones, stalactites, stalagmites). Depending on the prevalent type of accretion, especially in the proximity of the speleothem surface, the resulting form of the speleothem can also be intermediate between a massive and a coralloid type (Stepanov, 1997). Many stalagmites or stalactites, including stalagmites used in paleoclimate research (Fairchild and Baker, 2012), are indeed intermediate forms, because they show a complete or partial corrugated surface and consist of assemblages of smoothing and coralloid accretions (Fig. 2e and f).

To explain the cause of the growth pattern of coralloids and its deviance from that observed in massive speleothems, various hypotheses have been advanced. Coralloids can form both subaerially and subaqueously and, in theory, by different mechanisms. Subaqueous deposition of coralloids seems comparatively straightforward, in that the source of constituents surrounds the growing speleothem. On the other hand, subaerial deposition of coralloids in the absence of standing or flowing water is more problematic and has been explained by two very different mechanisms. One is deposition from aerosols, either as solid material (Cser and Maucha, 1968; Klimchouk et al., 1995; Dublyansky and Pashenko, 1997) or as hydroaerosols from splashes (Perna, 1989), wherein the tips of coralloids grow faster because they are fed by aerosol particles coming from a wider angular range compared to the reentrant parts of the coralloids' surface (Fig. 3a). The second is deposition from a thin capillary film of supersaturated solution (Serban et al., 1961; Moroshkin, 1976; Maltsev, 1993, 1994, 1997; Stepanov, 1997, 1999; Self and Hill, 2003). This solution could have, in turn, various sources that include splash effects of dripping water (Balch, 1948), seepage through the cave bedrock, and condensation (Stepanov, 1999). The latter could result from cycles of condensation and evaporation (Istvan and Micle, 1994).

Dawkins (1874) already concluded that coralloids start to grow from a slight elevation of the substrate, probably because of greater evaporation of water there than from the surrounding recessive portions. Thrailkill (1965) attributed the origin of cave popcorn to the deposition of $CaCO_3$ mainly driven by CO_2 loss from a thin film of solution. Slyotov (1985) identified a geometric advantage for protruding regions to grow by mass transfer with the medium. If, along the mass transfer pathway between a point on a growth surface and the air, there is another growth surface which can lose H_2O or CO_2 molecules from its capillary film, the two surfaces exchange an amount of these molecules and thereby inhibit each other's growth by increasing the concentration of H_2O or CO_2 molecules in the intervening space. This effect, of course, should be greater as the two branches of coralloids approach each other. According to Slyotov (1985), this is why a gap is sustained between the two surfaces, rather than a joining of the two (Fig. 3b).

In light of the apparent importance of solute supply and substrate control to the hypothesized origins of the various kinds of speleothems, this

paper reports measurements of $\delta^{13}C$ and $\delta^{18}O$ from samples positioned sequentially along growth layers (accretions) in various speleothems. These measurements allow estimation of the varying extent of degassing and evaporation from water moving across the speleothems, and thus allow evaluation of the hypothesized origins of these varied speleothems, and especially of coralloids.

2. Speleothems studied

To compare isotopic characteristics of coralloid and smoothing accretions, we analyzed subaerial coralloids, subaqueous coralloids, a stalactite on which coralloids have formed, a flowstone, and a stalagmite with coralloids on its flanks. With the exception of the last one, these speleothems come from Is Zuddas Cave in Sulcis, the southwestern region of the Mediterranean island of Sardinia, the more northwestern of Italy's two large islands. The cave lies in dolomitized carbonate rocks of the Lower Cambrian Gonnesa Group (Bechstadt and Boni, 1996). This cave is about 1500 m long and is characterized by a succession of rooms connected by narrow natural tunnels. In this cave a wide variety of speleothem types has been identified, including flowstones, stalactites, stalagmites, subaerial and subaqueous coralloids, pool spar, frostworks, helictites and many others (Caddeo et al., 2008a, 2008b). Designations of these speleothems all begin with "IZ" for "Is Zuddas".

The stalagmite with coralloids on its flanks, which comes from the collection of Prof. George A. Brook of the University of Georgia (U.S.A.), was collected from Drotsky's Cave, located in the Gcwihaba Hills of the Ngamiland District of northwestern Botswana, within the Kalahari Desert (Africa). Drotsky's Cave is a little over 400 m long and lies in dolomitic marble of the upper Proterozoic Otavi Group or Damara Sequence (Railsback et al., 1994). Speleothems observed in this cave are most commonly stalactites and stalagmites, and the stalagmites like the one studied here have locally been coated with subaerial coralloids. The designation for this stalagmite begins with "DR" for "Drotsky's".

3. Methods and materials

Powders were drilled from sequential locations along the stratification of the layers in 6 speleothems. Layers were selected for (i) homogeneity, with no variation in mineralogy along the layer; (ii) sufficient distinction to allow clear identification; and (iii) sufficient thickness for extraction of samples. The latter is problematic because layers in coralloids are commonly very thin in the reentrants between projections. Powders for X-ray diffraction (XRD) and isotopic analyses were sampled using a dental drill. Cutting of the speleothems, preparation of thin sections, and optical studies by conventional petrographic microscope were performed both at the Department of Chemical and Geological Sciences of the University of Cagliari (Sardinia, Italy) and at the Department of Geology of the University of Georgia (Athens, Georgia, USA). The mineral phases were also determined (Table 1) at both departments, respectively using an X-ray diffractometer Panalytical X'Pert Pro, operating at 40 mA and 40 kV with monochromatic CuKα radiation, and a Scintag X-ray diffractometer operating at 40 mA and 40 kV with monochromatic CoKα radiation.

Carbon and oxygen stable isotope analyses were performed at the Department of Geology of the University of Georgia (Athens, USA) by a method modified from McCrea (1950). About 5 mg of powder for each analysis point was reacted under vacuum in 100% phosphoric acid at 50 °C. The resulting CO_2 was extracted on a conventional vacuum line and analyzed on Finnigan MAT Delta E and MAT 252 mass spectrometers. Laboratory standards were prepared and analyzed with each batch of samples. Standards have been calibrated to NBS 19 ($\delta^{13}C = +1.95$, $\delta^{18}O = -2.2‰$ relative to VPDB) and NBS 18 ($\delta^{13}C = -5.0$ and $\delta^{18}O = -23.0‰$ relative to VPDB). Isotopic results are normalized to the lab standards using a two-point scale, so that all $\delta^{13}C$ and $\delta^{18}O$ values herein are reported relative to VPDB. The 2 sigma error of the combined extraction and analysis is 0.04‰ for $\delta^{13}C$ and 0.05‰ for $\delta^{18}O$.
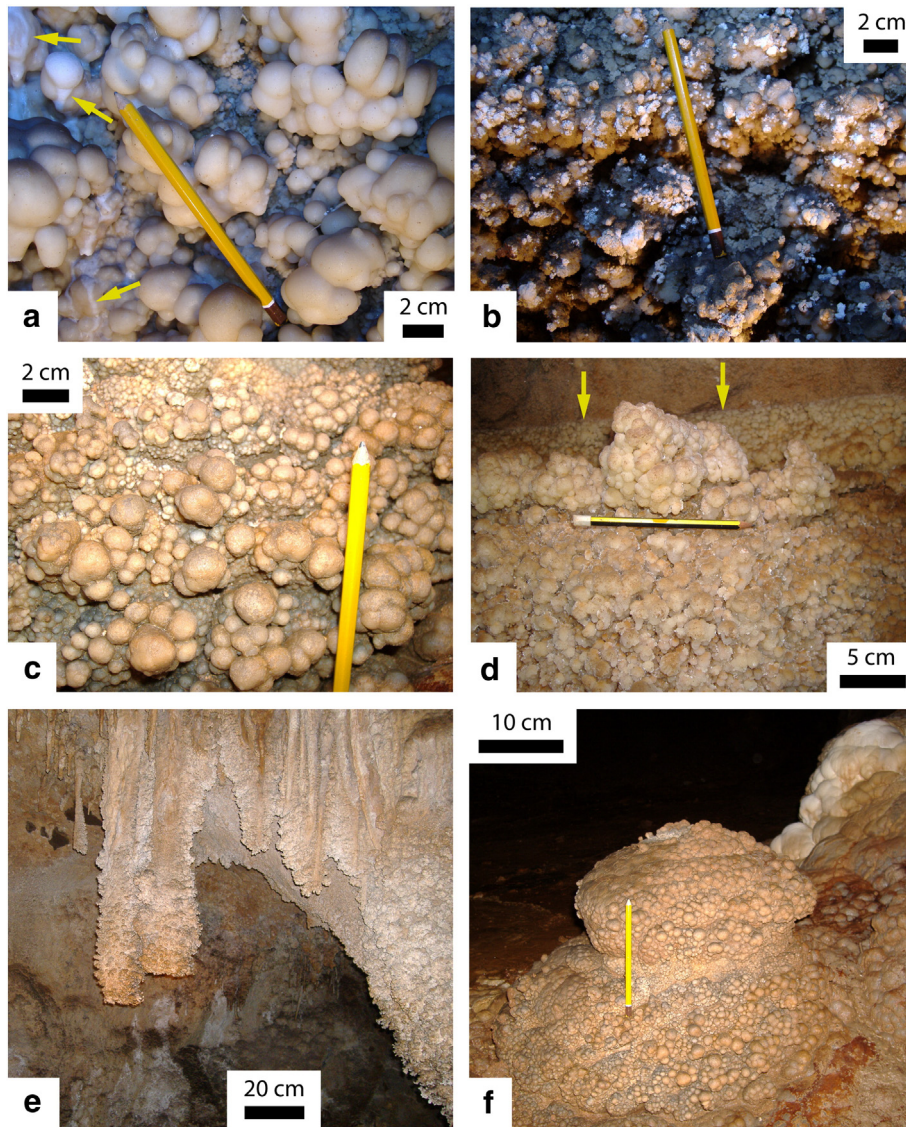
Fig. 2. A variety of coralloids in Is Zuddas Cave (Sardinia, Italy). (a) Subaerial coralloids growing from a wall. Note some evidence of water flowing by gravity along the wall where subaerial coralloids form (arrows). (b) Subaerial coralloids growing from a wall. The white substance on the coralloids' surface is moonmilk of metastable huntite which usually forms as product of extreme evaporation. Similar white deposits are also visible along the section of a studied specimen (Fig. 8a) where they consist of secondary protodolomite. (c) Subaerial coralloids growing on a floor. In this case the supply solution probably feeds the coralloids by a splash effect. (d) Subaqueous coralloids inside an almost-drained pool. The old level of the water table in the pool is well evident and marked by two arrows. (e) Stalactites consisting of assemblages of smoothing and coralloid accretions, which are locally coated by coralloids. Note that coralloid crusts tend to increase their thickness in the lower parts of both stalactites and wall, probably because of a more frequent occurrence of capillary water. A preferential development is also evident in more evaporative sides of some stalactites. (f) Stalagmite consisting of assemblages of smoothing and coralloid accretions, which is locally coated by coralloids.
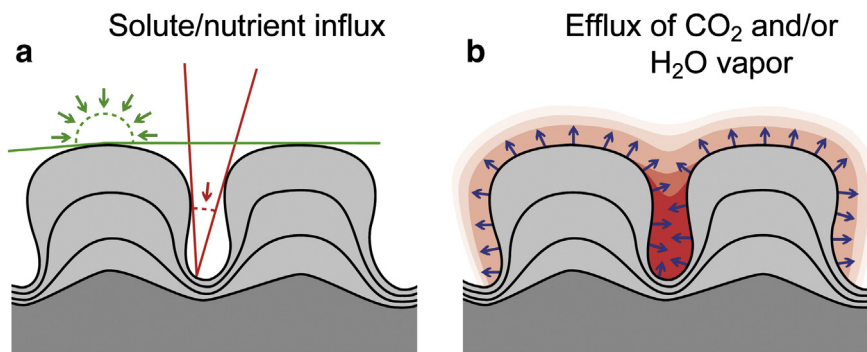

Fig. 3. Models previously proposed to explain the morphology of coralloids, which have layers thicker on outer margins and thinner between them. (a) Greater angular range at tips of coralloid (broader angle) than on recesses between coralloids (smaller angle) allowing greater aerosol or hydroaerosol flux to tips of subaerial coralloids and thus faster growth in more exposed areas. (b) Flux of CO_2 away from tips of coralloids, leading to mutual suppression of growth on flanks of coralloids with CO_2 trapped between them (an indirect competition). Both models (a and b) favor faster growth on tips of coralloids and thus toward free space.

4. Results

4.1. Overview of results

The values of $\delta^{13}C$ and $\delta^{18}O$ measured in the speleothems examined in this study vary greatly, with $\delta^{13}C$ varying from -9 to $+6‰$ relative to the VPDB standard and $\delta^{18}O$ varying from -8 to $0‰$ relative to VPDB (Fig. 4). The resulting ranges, 15‰ for $\delta^{13}C$ and 8‰ for $\delta^{18}O$, exceed those commonly seen in other studies of multiple kinds of speleothems from a single cave (Fig. 4). The speleothems examined in this study show a positive correlation between $\delta^{13}C$ and $\delta^{18}O$, both collectively and with regard to all of the individual speleothems studied, other than the subaqueous coralloids (Fig. 4).

4.2. Flowstone

Speleothem IZFL is a piece of a long flowstone that covers tens of square meters of the sloping irregular floor in the first room of Is Zuddas Cave. The piece was detached with explosives by quarrymen in 1968, but its shape is sufficiently distinct to allow inference of its original position and thus the direction of the flowing water from which it formed. In the laboratory, the flowstone was cut along the line of greater slope and along the direction of flow of the precipitating water. Samples for stable isotope analysis were taken along a smoothing accretion of pale gray calcite that shows no change in thickness corresponding to the substrate morphology. Where possible, samples were positioned to alternate between prominences and recesses of the underlying substrate (Fig. 5a).

The ranges of both $\delta^{13}C$ and $\delta^{18}O$ in this flowstone layer are small (0.6‰ and 0.4‰, respectively) compared to ranges of isotopic composi tions of other speleothems examined in this study (Fig. 4). Between adjacent points, differences are only 0.0 to 0.3‰ (Fig. 5b). Slightly larger variations can occur between more distant points, up to 0.6‰ for $\delta^{13}C$ and 0.4‰ for $\delta^{18}O$. Thus, in this speleothem there is no evident control on C or O isotopic composition by the substrate morphology. More interestingly, both $\delta^{13}C$ and $\delta^{18}O$ increase in the direction of water flow: the mean $\delta^{13}C$ and $\delta^{18}O$ for the six most downstream samples are $-6.69‰$ and $-3.30‰$, respectively, whereas the mean values in the six most upstream samples are $-6.92‰$ and $-3.49‰$ (Fig. 5b). This enrichment in ^{13}C and ^{18}O in the direction of flow can be explained by degassing of CO_2 and simultaneous evaporation of H_2O during the movement of water from upstream to downstream, and thus by the evolution of individual units of water during its flow downstream.

4.3. Stalactite with coralloids

Speleothem IZST, which was found on the floor of Is Zuddas Cave, is a fragment of a stalactite on which coralloids have formed. The speleothem was cut along a longitudinal section, following the axis of the stalactite. Because the specimen is a stalactite, the downward flow direction of the original feeding water is clearly known (Fig. 6a). Coral loid accretions are visible, but none of them were sufficiently thick and homogeneous for sampling. Instead, four stable isotope analyses were performed on a smoothing accretion of gray and pure calcite developed on a very corrugated substrate. One analyzed location, S3, is on a prom inence, whereas S2 and S4 are located in adjacent concavities (Fig. 6a).

The ranges of both $\delta^{13}C$ (1.0‰) and $\delta^{18}O$ (0.7‰) in this smoothing accretion are greater than those observed in the Flowstone IZFL. Values of $\delta^{13}C$ and $\delta^{18}O$ show a positive correlation, and both $\delta^{13}C$ and $\delta^{18}O$ increase in the direction of water flow, suggesting both degassing and evaporation over time as the solution moved down the stalactite (Fig. 6b). Both $\delta^{13}C$ and $\delta^{18}O$ reach their maxima on the prominence (Point S3) and are greater by 0.69‰ and 0.46‰, respectively, compared to those at Point S2. Fractionation at S3 is also greater than S4 despite the fact that a gravity effect should favor greater values at the down stream point. Thus, in this speleothem, convex topography of the

substrate has an effect on isotopic composition. The substrate also seems to affect the change in isotopic composition between Points S1 and S2, even if $\delta^{13}C$ and $\delta^{18}O$ increase from a prominence (S1) to a concavity (S2). This is because, if the increase from S1 to S3 were only due to the gravity, the values at S2 would presumably be the means of the values at S1 and S3. However the values at S2 are less than those means. This shows that the values of $\delta^{13}C$ and $\delta^{18}O$ at S2 are the result not only of gravity control but also of substrate control.

Compared to Flowstone IZFL, Specimen IZST displays greater in creases in $\delta^{13}C$ and $\delta^{18}O$ in the direction of water flow and shows more the marked increases in $\delta^{13}C$ and $\delta^{18}O$ on the substrate's prominences. This amplification of effects in Specimen IZST, the stalactite on which coralloids have formed, may be the result of a lesser flow rate of the nurturing solution over the stalactite than over the flowstone.

Table 1
Mineralogy (Cc = calcite, Ar = aragonite) and stable isotope data reported in ‰ vs. VPDB, relative to the six analyzed specimens.

Speleothem type	Specimen	XRD	Sample	$\delta^{13}C$	$\delta^{18}O$
Flowstone	IZFL	Cc			
			F1	6.83	3.52
			F2	6.92	3.36
			F3	7.08	3.64
			F4	6.82	3.40
			F5	6.88	3.49
			F6	6.96	3.51
			F7	6.79	3.35
			F8	6.92	3.37
			F9	6.81	3.37
			F10	6.83	3.35
			F11	6.47	3.25
			F12	6.54	3.26
			F13	6.59	3.21
Stalactite	IZST	Cc			
			S1	4.56	5.45
			S2	4.26	5.23
			S3	3.57	4.77
			S4	3.89	5.03
Stalagmite	DRSG	Cc			
			G1	6.80	7.10
			G2	7.30	7.55
			G3	7.50	7.65
			G4	7.70	7.85
			G5	7.20	7.80
			G6	6.70	7.50
			G7	6.30	7.00
			G8	4.90	5.90
			G9	5.90	6.70
			G10	6.70	7.20
			G11	6.50	7.30
			G12	4.50	5.50
			G13	5.14	5.77
			G14	4.03	4.85
			G15	3.90	4.89
			G16	6.33	6.74
Subaerial coralloids	IZAC	Ar			
			A1	5.47	0.28
			A2	4.73	0.29
			A3	3.80	0.41
			A4	4.54	0.39
			A5	5.15	0.42
			A6	5.90	0.23
			B1	5.31	0.05
			B2	4.51	0.47
Subaqueous coralloids	IZWC1	Cc			
			C1	8.07	4.15
			C2	7.96	4.60
			C3	8.07	4.47
			C4	8.10	4.12
Subaqueous coralloids	IZWC2	Cc			
			D1	9.67	5.37
			D2	9.47	5.32
			D3	9.49	5.37
			D4	9.44	5.15

4.4. Stalagmite with coralloids on its flanks

Stalagmite DRSG, which was collected for paleoclimate study (Railsback et al., 1994), was cut along a longitudinal section containing the stalagmite axis. Most layers of the stalagmite have a smooth crest, but some become more corrugated on the stalagmite's flanks to give coralloid forms there. Sixteen points were analyzed along one smoothing accretion of white calcite from the stalagmite's crest to its flank, with samples from both prominences and concavities. Because the sample is a stalagmite, the downward flow direction of the original feeding water is clearly known, from sample G1 to G16 (Fig. 7a).

Values of $\delta^{13}C$ and $\delta^{18}O$ along the smoothing accretion have large ranges (3.8‰ and 3.0‰, respectively), and together they show a strong positive correlation (Fig. 7b). Like the smoothing accretions in Speleothems IZFL and IZST, the analyzed smoothing accretion of the Stalagmite DRSG exhibits enrichment in heavy isotopes in the direction of liquid movement (Fig. 7b). In addition, as in Stalactite IZST, substrate morphology controls isotopic composition. For example, rela tive maxima of both $\delta^{13}C$ and $\delta^{18}O$ at Points G8, G12 and G15 are located on the highs of the substrate, whereas relative minima of $\delta^{13}C$ at Points G10, G13 and G16 and relative minima of $\delta^{18}O$ at Points G13 and G16 are located in lows (Fig. 7a and b). Thus, except the value of $\delta^{18}O$ in the point G11, all relative maxima are in protruding zones and all relative minima are in recesses of the substrate. In general, Fig. 7 shows a good correspondence between the morphology of the substrate and isotopic composition. Of course, some local effects can also affect the isotopic com position, distorting a little its pattern with respect to the substrate morphology. For example, in each protruding zone the downstream side is always more enriched in heavy isotopes than the upstream one, suggesting a greater exposure to an air current in that side. This is also shown by the preferential growth direction of some coralloids formed on the flank of the stalagmite (see arrows in Fig. 7a). To summarize, iso topic compositions in this specimen seem to be controlled by a gravity effect, a substrate effect, and a third factor, an effect resulting from air flow, which may have been accentuated because of the position of Stalagmite DRSG near the entrance of the cave.

4.5. Subaerial coralloids

Specimen IZAC of subaerial coralloids formed on a wall along a corridor between two larger rooms of Is Zuddas Cave. The specimen was first cut along a plane containing the growth direction and passing through two branches (Fig. 8a). The resulting section, designated as Section A, shows a sequence of coralloid accretions. Alternating with layers of aragonite and Mg calcite in this section are some white pseudoaggregates of protodolomite (Fig. 8a). The morphology of the pseudoaggregates suggests that the protodolomite formed by replace ment of some metastable minerals of an original moonmilk. Moonmilk is a white and soft substance formed as the final product of evaporative sequences, because it precipitates from very residual and Mg rich solutions (Cabrol, 1978). In Is Zuddas Cave, moonmilk consists prevalently of Mg carbonates huntite or hydromagnesite (Caddeo, 2011) and it is readily visible on the surface of some growing subaerial coralloids (Fig. 2b). Thus the metastable minerals of moonmilk are probably the pre cursors of the pseudoaggregates of protodolomite recognized in the Spec imen IZAC. The recrystallized moonmilk is a potentially important clue in understanding the genesis of the Subaerial Coralloids IZAC.

Stable isotope analyses along one coralloid accretion of parallel acicular aragonite needles reveal very high values of $\delta^{13}C$ (+3.8 to +5.9‰ relative to VPDB) and $\delta^{18}O$ (−0.4 to almost 0‰ relative to VPDB), much higher than those measured in common speleothems (Fig. 4). Values of $\delta^{13}C$ vary with position along the accretion, with the greatest on the protrusions of the coralloids, where the accretion is thickest (Samples A1 and A6 in Fig. 8a and c), and least in the recesses, where the accretion is thinnest (Samples A2 to A4). The same relationship of thickness and isotopic composition can be seen in a second section, designated as

Section B, where both $\delta^{13}C$ and $\delta^{18}O$ are greater in Sample B1 than in Sample B2 (Fig. 8b and c).

4.6. Subaqueous coralloids

Subaqueous coralloids designated as IZWC1 (Fig. 9a) and IZWC2 (Fig. 9b) were collected from two different rooms in Is Zuddas Cave. They were located in two pools, above the present water levels of each. In these pools, the upper boundaries of the coralloids are marked by even horizontal lines (Fig. 2d) at the same level as nearby shelfstones. Thus, those upper boundaries mark old levels of the water surface in the pool, under which coralloids formed in the past. Specimen IZWC1 formed from a submerged wall (Fig. 2d), but Specimen IZWC2 formed on some submerged stalactites, as the horizontal section in Fig. 9b shows. Growth had ceased in both coralloids when they were collected.

Specimens IZWC1 and IZWC2 both consist of sequences of coralloid accretions of calcite, with crystals perpendicular to the substrate be cause of geometric selection (Grigor'ev, 1961). The variation of thick ness in synchronous deposits in these subaqueous coralloids is similar to the pattern variation in subaerial coralloids. However, these subaque ous coralloids do not have large values of $\delta^{13}C$ and $\delta^{18}O$ (not exceeding

−7.9‰ and −4.1‰, respectively). Furthermore, $\delta^{13}C$ and $\delta^{18}O$ show little variation within individual accretionary laminae and thus show little response to the morphology of the substrate (Fig. 9c).
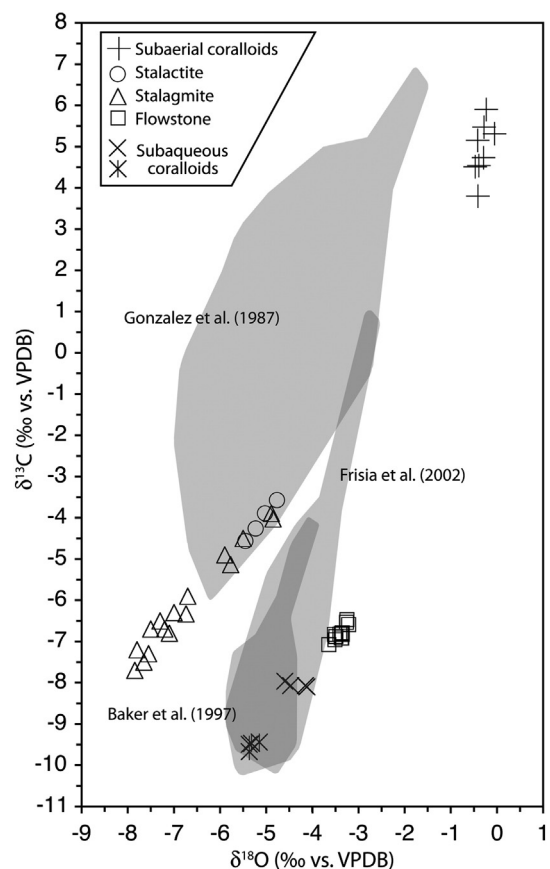

Fig. 4. Carbon and oxygen isotope composition of all samples from the six specimens analyzed in this study. Gray fields represent data obtained in other stable isotope studies of assorted speleothems (Gonzalez and Lohmann, 1988; Baker et al., 1997; Frisia et al., 2002). Note the large difference in the isotopic composition between subaerial coralloids (Specimen IZAC) and the other types of speleothems, including subaqueous coralloids.
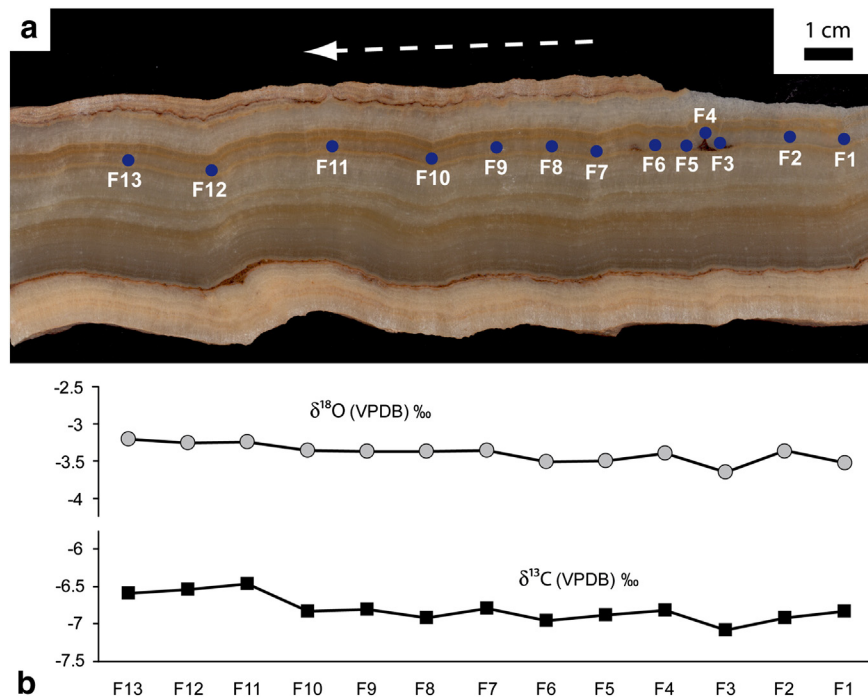
Fig. 5. (a) Section of the Flowstone IZFL, cut along the original water flow direction, which is indicated by the dashed arrow. Circles indicate the points in a smoothing accretion of calcite from which powders were sampled by a dental drill for stable isotope analysis. (b) Variation in $\delta^{13}C$ and $\delta^{18}O$ along one smoothing accretion of the Flowstone IZFL.

4.7. Synthesis of isotopic results

Taken together, the data reported above show a consistent relationship between $\delta^{13}C$ and the extent of substrate control. If the difference between $\delta^{13}C$ of prominences and adjacent recessed areas ($\Delta\delta^{13}C$) is used as a measure of substrate control on isotopic composition, then the extent of substrate control is strongly correlative with enrichment in ^{13}C in the speleothems from Is Zuddas Cave (Fig. 10). Both parameters prog ress from subaqueous coralloids, precipitated in water of pools, where maximal values of $\Delta\delta^{13}C$ are only 0.1 to 0.2‰ and $\delta^{13}C$ in recesses is -8.0 to -9.5‰ relative to VPDB, to flowstones and stalactites precipitated from films of flowing water, and finally to subaerial coralloids, presum ably precipitated from capillary waters, where maximal values of $\Delta\delta^{13}C$ are 2.2‰ and $\delta^{13}C$ in recesses is $+3.8$‰ relative to VPDB. Both parameters thus seem to show a pronounced relationship to the abundance and behavior of the waters from which precipitation occurred, with greatest values in the least abundant and slowest moving water.

Another common characteristic in the data reported above is an increase in $\delta^{13}C$ and $\delta^{18}O$ in the direction of flow for the three studied smoothing accretions in which flow is relevant (the flowstone, stalactite, and stalagmite) (Fig. 11). This trend is least evident in the flow stone, where water was probably most abundant, and most evident on the flanks of the stalagmite, where water was probably least abun dant. Positive excursions within these trends are evident at promi nences in the speleothems' surfaces (Fig. 11).

5. Discussion

5.1. A model for solution transfer in the growth of subaerial speleothems

To account for both the increase in $\delta^{13}C$ and $\delta^{18}O$ in the direction of flow and the localized increase in those parameters at prominences on smoothing accretions (from flowstone, stalactite, and stalagmite), one can envision the supply of water on the speleothem surface as a succession of many inputs. These inputs range between two end members. In one end member, water is sufficiently abundant to flow by gravity,

during a "gravity stage" of deposition (Fig. 12a), and in the other water is sufficiently scarce that it forms a very slow moving capillary film, during a "capillary stage" (Fig. 12c). During gravity stages the solution becomes richer in ^{13}C and ^{18}O with increasing distance from the water source and increasing degassing and evaporation, but flow makes the solution uniform over prominences and recesses. On the
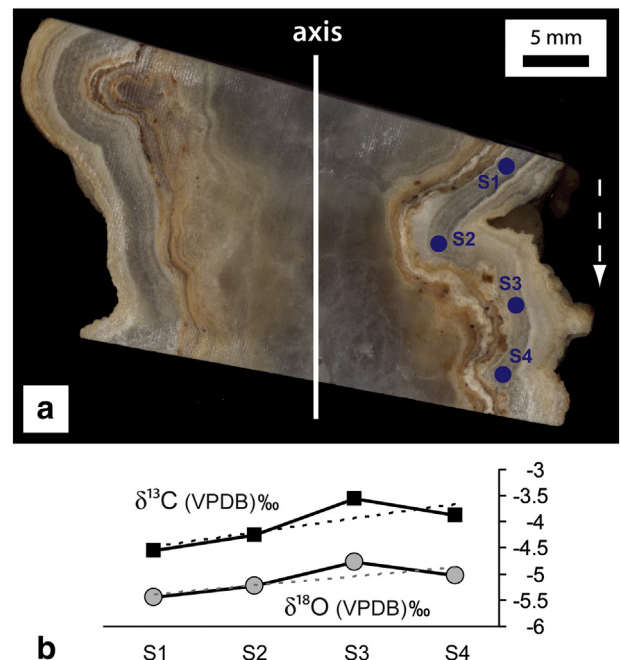

Fig. 6. (a) Longitudinal section cut along the axis of the Stalactite IZST. The dashed arrow indicates the general flow direction of the feeding water. Circles indicate the locations along one smoothing accretion of samples for stable isotope analysis. (b) Variation in $\delta^{13}C$ and $\delta^{18}O$ along the studied smoothing accretion of the Stalactite IZST; dashed lines indicate the overall linear trends of the data, illustrating the variation in isotopic composition along the overall direction of the water flow.

other hand, during capillary stages the solution becomes more enriched on prominences of the spelean surface, for at least two possible reasons. Firstly, faster water evaporation on the prominences induces water to move from the depressions toward the tips (Badino et al., 2011), where water arrives more enriched than in the surrounding zones. Secondly, if degassing and evaporation are greater from the promi nences, kinetic fractionation is also greater in those areas. Thus the signature of gravity stages in a deposit is the trend of increasing $\delta^{13}C$ and $\delta^{18}O$ with distance from the water source, whereas the signature of capillary stages is relative maxima of the $\delta^{13}C$ and $\delta^{18}O$ on the substrate protrusions.

In the continuum between gravity and capillary stages, one can further envision an intermediate mode of water movement in which gravity flow predominates between protrusions but capillary movement occurs toward prominences (Fig. 12b). Intermediate stages can explain the coexistence of gravity and capillary control in the smoothing accretions of Stalactite IZST and Stalagmite DRSG. Stages nearer the gravity end of the continuum would favor filling re-entrants with smoothing accretions, giving to the speleothem an overall massive form, in part because the material needed to enhance a concave surface is less than that needed to enhance a convex one. On the other hand, stages nearer the capillary end of the continuum would enhance the topography of the surface, because in that case the deposition rate seems mostly controlled by localized degassing and/or evaporation, rather than the supersaturation in background. This is supported by Fig. 10, where the parameter that quantifies the extent of the substrate

control ($\Delta\delta^{13}C$) is strongly correlated with both the decrease in water availability and with $\delta^{13}C$, which can be assumed as a measure of an increasingly evolved and less supersaturated solution. Among the subaerial speleothems studied here, Flowstone IZFL would have resulted mostly from gravity stages, whereas Subaerial Coralloids IZAC by a dom inance of capillary stages. On the other hand, the sequence of smoothing and coralloid accretions in Stalagmite DRSG and Stalactite IZST could be explained by alternation between two conditions, one in which fluctua tion between gravity and intermediate stages prevails and another in which fluctuation between intermediate and capillary stages prevails.

The continuum from gravity to intermediate to capillary stages, the predominance of which can change through time, thus explains how speleothems with an earlier overall smooth surface can become coated with coralloids (see Fig. 2e and f). More generally, it provides a unifying model of the growth of massive, corolloid and intermediate forms of subaerial speleothems. The growth of coralloid accretions during some intermediate stages is also possible and would explain the genesis of hybrid speleothems, which are a particular case of intermediate forms (Stepanov, 1997). These have been described as a sort of coralloids growing in a constant intermediate stage, during which a residual gravitational control persists through time.

5.2. The genesis of subaerial coralloids in capillary stages

Several lines of evidence from Specimen IZAC support the genesis of subaerial coralloids from capillary stages. Firstly, the correlation of
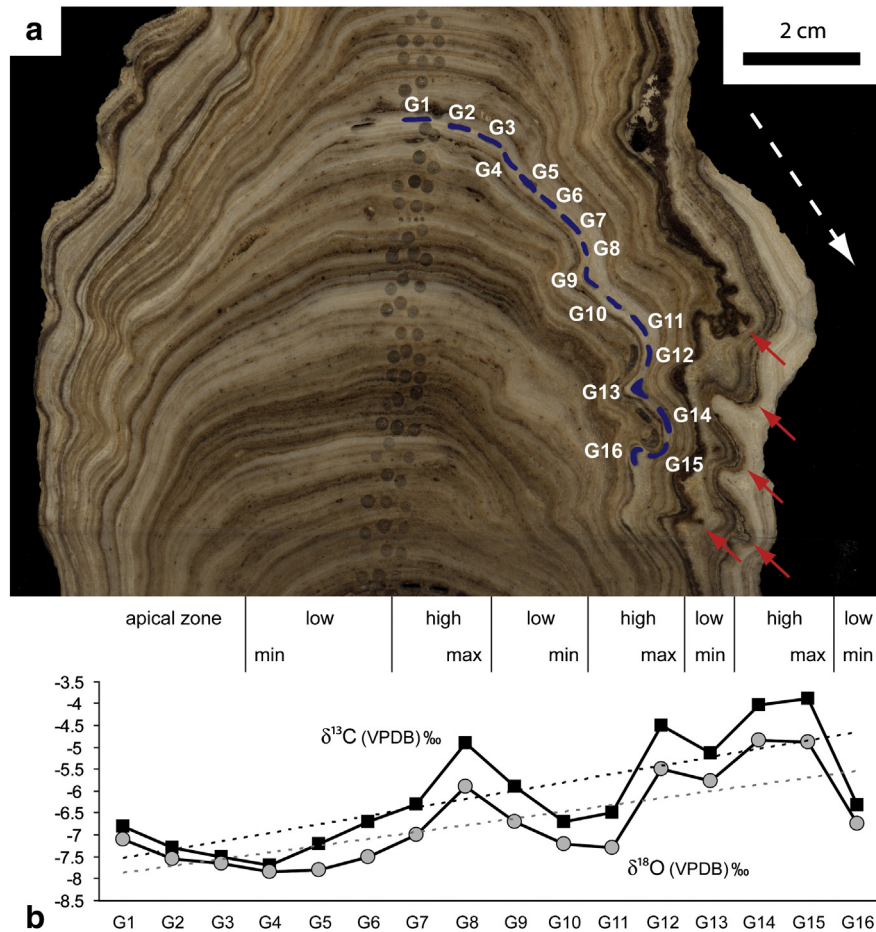

Fig. 7. (a) Longitudinal section along the axis of the Stalagmite DRSG. The labeled areas indicate the locations of samples for stable isotope data along a smoothing accretion of calcite. The dashed white arrow indicates the flow direction of water, solid red arrows indicate a possible prevalent air current direction favoring greater growth rate of coralloids and greater isotopic fractionation in the downstream side of the prominences. (b) Variation in $\delta^{13}C$ and $\delta^{18}O$ along the analyzed smoothing accretion of the Stalagmite DRSG. Dashed lines indicate the overall linear trends of the data, illustrating the variation in isotopic composition along the overall direction of the water flow. Labels above the plot show the good correlation between the substrate morphology (alternating highs and lows) and the isotopic composition pattern (alternating maxima and minima). (For interpretation of the references to color in this figure legend, the reader is referred to the web version of this article.)

substrate morphology, variation in thickness of accretions, and $\delta^{13}C$ (Fig. 8) indicate that the solution moved from the base toward the prominences of the subaerial coralloids, increasing both its depositional rate and fractionation along the way. Secondly, values of $\delta^{13}C$ and $\delta^{18}O$ from Specimen IZAC are by far the greatest found in this study (Fig. 4), suggesting that this speleothem was deposited from very evolved and fractionated solutions, highly affected by both CO_2 degassing and H_2O evaporation. Thirdly, the genesis of pseudoaggregates of moonmilk during the growth of the subaerial coralloids in Specimen IZAC (Fig. 8a) suggests that solids were deposited on the coralloids surface from very evolved Mg rich solutions, under extreme evaporative conditions (Gonzalez and Lohmann, 1988; Onac and Kearns, 2000). All these findings point to a very slow moving capillary film of solution.

Conversely, the relationship between $\delta^{13}C$ and substrate morphology in Specimen IZAC disproves the hypothesis of some authors that cor alloids form by deposition of solid particles from the air, as an aerosol, because it is very unlikely that aerosol particles having heavier C isotopes go only to the tips of coralloids, and that those having lighter C isotopes go to the rest of the surface. The hypothesis of aerosol depo sition is additionally disproved by the ordered structure of the aragonite aggregates, which consist of acicular crystals that are perpendicular to the substrate as the result of geometric selection (Grigor'ev, 1961). That pattern is very different from the disordered pseudoaggregates (Self and Hill, 2003) that are expected from aerosol deposition.

Coralloids like Specimen IZAC cover large portions of some walls as well as some stalactites and stalagmites in Is Zuddas Cave (Fig. 2a, b, e and f). However, along walls where coralloids formed, some evidence of flowing water is locally recognizable (Fig. 2a). This suggests that during some inputs, the rate of water supply was sufficient to favor movement by gravity in that zone, indicating flowing water as the original source of the feeding solution. This further supports the notion of a fluc tuating boundary between gravity, intermediate and capillary stages through time discussed above. However, the dominance of coralloids suggests that during most inputs, the solution arriving in that zone did not move anymore by gravity because of a strong reduction in volume due to extensive previous evaporation. Thus, during most inputs, a cap illary film existed on the coralloids and their base. Because of the differ ence in evaporation rate between the tips and the surrounding zones, solution moved on the coralloids from the base toward the promi nences, where the liquid path reached its terminus (Fig. 13).

5.3. Relationships between $\delta^{13}C$ and $\delta^{18}O$ in subaerial speleothems

Relationships between $\delta^{13}C$ and $\delta^{18}O$ differ between smoothing and coralloid accretions of the subaerial speleothems studied. The three smoothing accretions (from flowstone, stalagmite, and stalactite) show a consistent relationship between $\delta^{13}C$ and $\delta^{18}O$, with a slope of about 1 within each group, suggesting a strong correlation between CO_2 degassing and H_2O evaporation (Fig. 4). Modeling by Gat and Gonfiantini (1981) indicates that $\delta^{18}O$ increases sharply early in the evolution of a cave water, when most of the arriving liquid remains to flow onward (Fig. 14, left side). The covariance of low values of $\delta^{13}C$ and $\delta^{18}O$ observed in the smoothing accretions, both along flowpaths
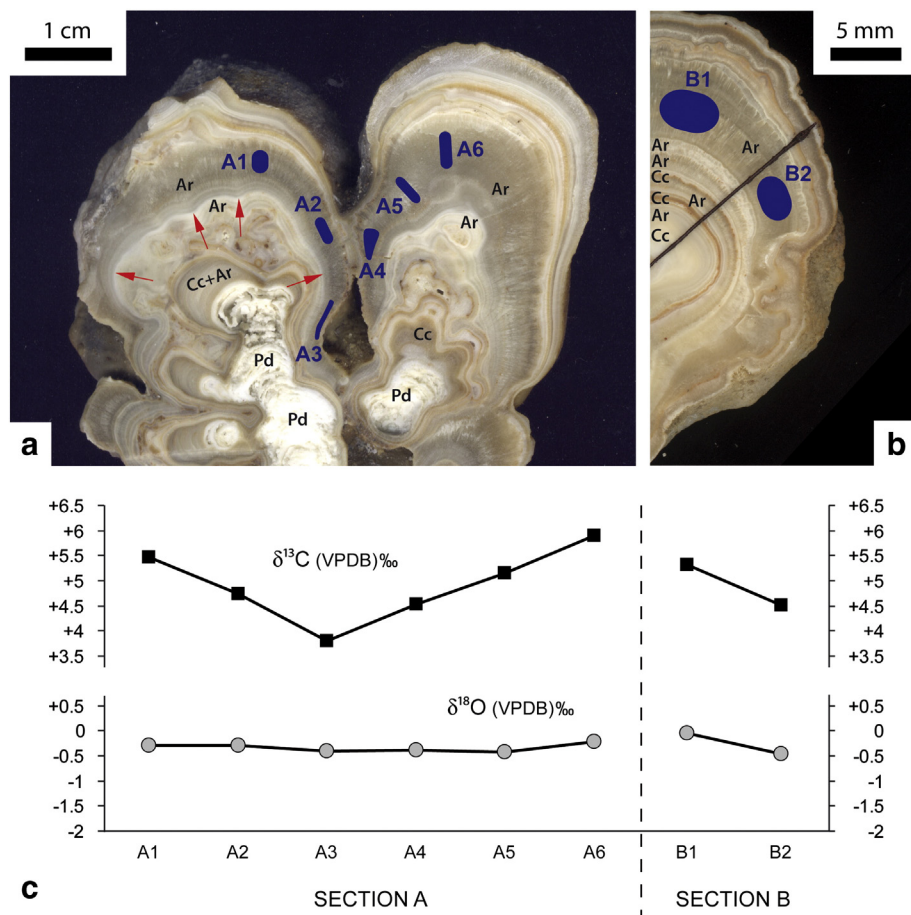

Fig. 8. Section A (a) and section B (b) of the Subaerial Coralloids IZAC. Marked and named areas indicate the points sampled for stable isotope data along one coralloid accretion of aragonite. Other labels indicate the mineralogically different layers (Cc = calcite, Ar = aragonite, Pd = protodolomite). Note that protodolomite has been found on various portions of recrystallized moonmilk. Arrows indicate some concavities and convexities located in protruding and sheltered zones, respectively, of the substrate. (c) Variation in $\delta^{13}C$ and $\delta^{18}O$ data from Section A and Section B of Specimen IZAC.
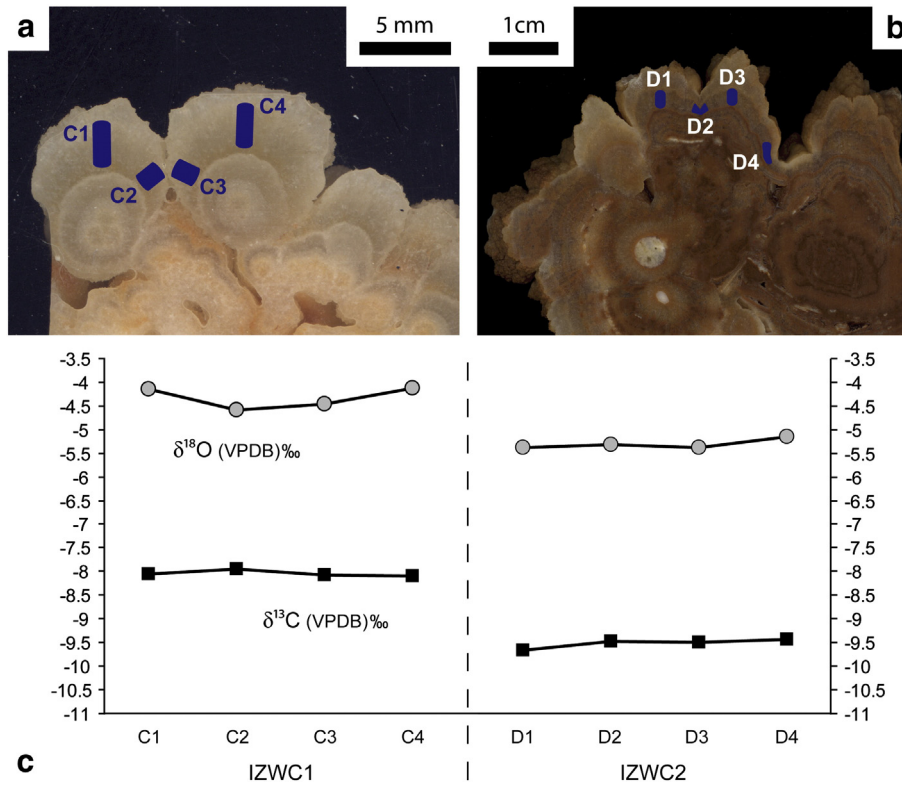
Fig. 9. Section of the Subaqueous Coralloids IZCW1 (a) and section of the Subaqueous Coralloids IZCW2 (b). Marked areas indicate the points sampled for stable isotope data along coralloid accretions of calcite. Both specimens have been cut along an originally horizontal plane. (c) Variation in $\delta^{13}C$ and $\delta^{18}O$ data from Specimens IZCW1 and IZCW2.

and in response to substrate prominences, therefore suggests both degassing and evaporation from little evolved waters moving over those speleothems.

Stable isotope data from the coralloid accretion of the Subaerial Coralloids IZAC differ from the data relative to the smoothing accretions in showing considerable variation in $\delta^{13}C$ but little variation in $\delta^{18}O$ (Fig. 8), even though the values of both are quite large (Fig. 4). This is an interesting result, in that deposition driven by extreme evaporation might be expected to result in extreme fractionation of oxygen isotopes. The modeling by Gat and Gonfiantini (1981) discussed above, however,

shows that when evaporation proceeds in an atmosphere with high humidity, like that of a cave, $\delta^{18}O$ of the water reaches a steady state value if a considerable amount of fluid has already been lost to evaporation (Fig. 14, right side). This would exactly be the case with subaerial coralloids, where capillary movement of previously evolved cave water reaches its terminus and cave humidity is high (humidity in Is Zuddas
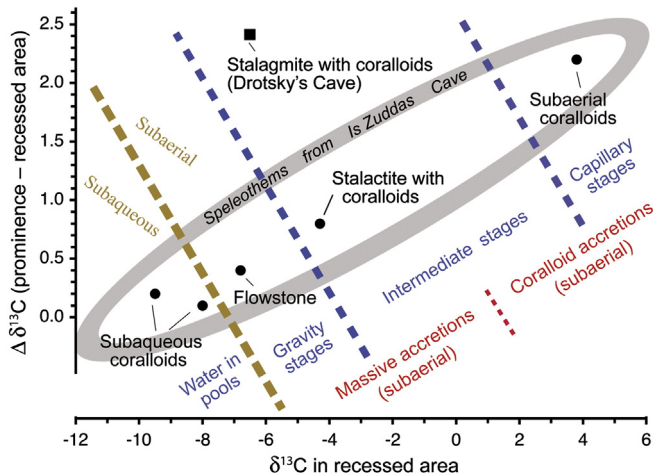

Fig. 10. Plot summarizing the carbon isotope data reported in this manuscript. For each accretion studied, the plot shows on the vertical axis the greatest difference in $\delta^{13}C$ between a prominence and a nearby recessed region, whereas $\delta^{13}C$ in that recessed region is shown on the horizontal axis. The gray shading encloses data from accretions from Is Zuddas Cave. The lines and labels indicate the conditions under which the different accretions formed and the resulting type of accretion.
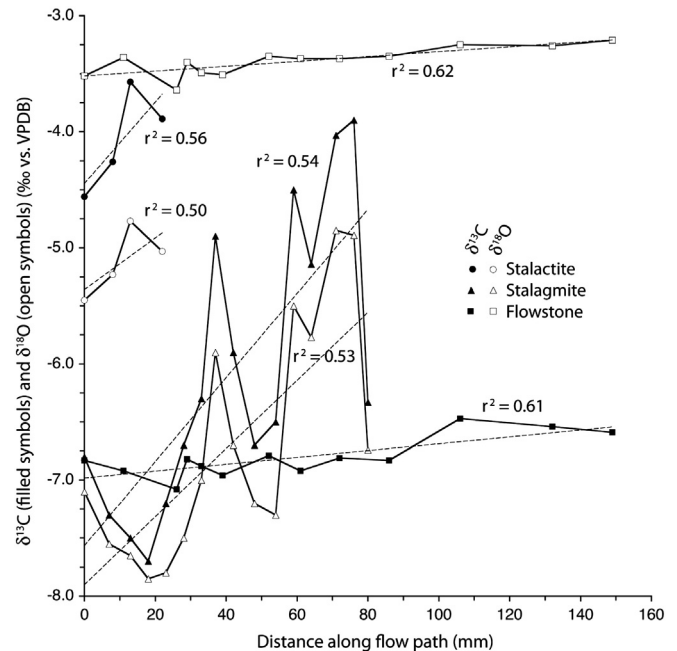

Fig. 11. Plot of $\delta^{13}C$ and $\delta^{18}O$ of smoothing accretions as a function of distance along the direction of flow of the precipitating water.

Cave ranges from 90% to 100%). This further supports our interpretation of subaerial coralloids as resulting from highly evaporated, and therefore capillary, water.

The very large values of $\delta^{13}C$, from $+3$ to $+6‰$ relative to VPDB, in subaerial coralloids may further reflect the importance of extreme evaporation in the formation of these digitate deposits. In most spelean waters, the rate of CO_2 degassing decreases quickly over time, and an evolved solution tends to be already saturated and equilibrated with respect to pCO_2, especially in a very thin capillary film (Dreybrodt, 1980, 1981). Evaporation, in contrast, can continue over time, and it can increase the saturation state of the solution, especially in advanced stages of evolution (Gonzalez and Lohmann, 1988). In subaerial coral loids, greater growth rate on tips of protrusions suggests that evapora tion causes greater supersaturation there. This process may explain the very high values of $\delta^{13}C$ in subaerial coralloids and especially on their tips because, in a solution saturated with respect to calcium carbonate, evaporation removes water molecules and concentrates the solutes. The increase in concentration can lead to precipitation of calcite or aragonite after the solubility product is surpassed (Appelo and Postma, 1993). Calcium carbonate precipitation occurs by the reaction:

$$Ca^{2+} + 2HCO_3^- \rightarrow CaCO_3 + CO_2 + H_2O$$
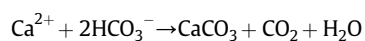
so that for each mole of deposited $CaCO_3$, one mole of CO_2 is created and the excess of CO_2 must degas from the solution (Dreybrodt, 2008). In this case the driving process for CO_2 degassing is precipitation of $CaCO_3$ which depends, in turn, on the evaporation. Thus, with continuing evaporation, resultant precipitation of $CaCO_3$, and resultant precipitation driven degassing, fractionation of ^{13}C can increase continuously in the residual solution, leading to values of $\delta^{13}C$ much greater than those found in $CaCO_3$ deposited from less evolved waters.

5.4. Controls on mass transfer between a capillary film and the air

The results discussed above suggest that differences in evaporation rate between tips and recesses of subaerial coralloids seem to be the key mechanism in the growth of those speleothems. The data further allow evaluation of two models accounting for differential evaporation, one depending on substrate curvature and the other on the more gener al form of the substrate.

The first of these models is that expressed by the Kelvin equation (Badino et al., 2011), where the natural logarithm of the ratio of actual vapor pressure to vapor pressure of a liquid at saturation is inversely proportional to the radius of curvature of the surface of that liquid. Thus evaporation is greater from a more tightly curved surface. Because the tips of coralloids, where coralloid accretions are typically thickest, have a comparatively small radius of curvature, the relationship expressed by the Kelvin equation would seemingly hold in the deposi tion of coralloids. However, the physical process characterized by the Kelvin equation is not adequate to explain the genesis of the Subaerial Coralloids IZAC (Fig. 8a). The substrate curvature in this specimen is large at greater scale, and some small variations of lesser magnitude are readily recognized at a smaller scale. For example, some local small concavities are recognizable on the protruding zones of the branches, and in the depressed zones some small convexities are appar ent (see arrows in Fig. 8a). Despite this, the thickness of the aragonite coralloid accretion is always greater in the small concavities of protrud ing zones than on the convexities of the depressed ones. This means that variation in thickness does not follow the detailed concavities and con vexities of the substrate but instead follows the larger scale substrate variations. It therefore seems that the different growth rate along these coralloids is not controlled by the Kelvin equation.

Rather than a model dependent on radius of curvature, both the distribution of thickness of accretions and the stable isotope data in Fig. 8 suggest a model governed by gradual change in the air along the growth surface. Slyotov (1985) suggested that differences in both

evaporation and degassing between the protrusions and depressed zones can be explained by the presence of different sub environments in the air over the coralloids. In this model, the coralloid morphology itself induces heterogeneity in the air around the coralloids, because the recesses are slightly more isolated from the cave atmosphere than are the protrusions (Fig. 13). Even assuming that the relative humidity (RH) in the cave atmosphere is on average less than 100%, very near to the capillary film of solution a boundary layer of air has always a relative humidity equal to 100% (Clark and Fritz, 1997). Thus a gradient of RH exists in a transitional layer of air between the capillary liquid and the bulk of the cave atmosphere. Through this transitional layer, vapor diffuses from the capillary film to the cave atmosphere, perpendicularly to the iso humidity surfaces. As schematized in Fig. 13, these iso humidity surfaces have a shape depending on the vapor source mor phology, which is the capillary film with the same shape as the substrate. Fig. 13 shows that the diffusion of H_2O molecules occurs faster from the tips, above which the iso humidity surfaces are more closely spaced than above the reentrants. Fig. 13 also shows that in a given time, the total net amount of vapor lost from the liquid surface in a depressed zone is much less than that lost from a less extensive liquid surface in a protruding region.

The same reasoning also works where CO_2 degassing is the control ling variable. In this case the curves represented in Fig. 13 would describe the pattern of the pCO_2 variation above the subaerial coralloids. The analogous control of the substrate on CO_2 degassing and solvent evaporation helps explain why $\delta^{13}C$ is correlated with substrate shape in subaerial coralloids (Fig. 8), with greater $\delta^{13}C$ at the tips where degassing is more effective. The strong correlation of $\delta^{13}C$ with substrate shape in subaerial coralloids (Fig. 10) can thus be explained by a combi nation of three mechanisms: (1) degassing of CO_2 during movement of capillary water toward the tips of the coralloids, (2) greater evaporation at the tips and thus more carbonate precipitation and its required degassing of CO_2, and (3) greater degassing at coralloid tips into air less enriched in CO_2 than the CO_2 enriched air sequestered in the recesses between coralloids.

5.5. A model for the genesis of subaqueous coralloids

The constant values of $\delta^{13}C$ in our two specimens of subaqueous coralloids, IZWC1 and IZWC2, demonstrate that there was no difference in outgassing of CO_2 along the surface of these speleothems,
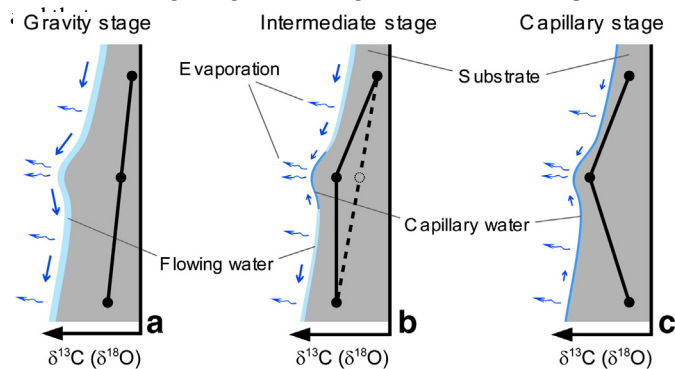

Fig. 12. Cross-sections showing idealized conditions of water films moving on the surface of a speleothem. These conditions include movement by gravity (a), capillary movement (c), and an intermediate condition (b) in which gravity control occurs on the re-entrant surfaces and capillary action moves water to prominences from which evaporation is enhanced. Note that changes in water supply through time will cause repeated changes among these three conditions. Thick solid black lines show variation in $\delta^{13}C$ and $\delta^{18}O$ along the deposited layer of calcium carbonate in three subsequent points, the second of which is on a prominence. Values are expressed with respect to the horizontal Cartesian axis at the bottom of the sketch, on which $\delta^{13}C$ and $\delta^{18}O$ increase to the left. For the central sketch, the dashed thick black line shows $\delta^{13}C$ and $\delta^{18}O$ variation considering a second point not in the prominence but in the adjacent re-entrant surfaces behind or in front of the plane of the sketch.

diffusion of CO_2 did not affect the isotopic composition of the solution near the speleothem. These data, combined with the subaqueous setting of these coralloids, show that deposition was not the result of transport by a capillary film, and more generally not the result of transport along the speleothem's surface. Thus the growth of these subaqueous coral loids had to involve transport from the surrounding medium beyond the spelean surface (Fig. 15) unlike the transport along the surface in ferred in subaerial coralloids (Fig. 13).

The growth of the subaqueous coralloids can be explained by different rates of diffusive feeding of solutes from the bulk solution to the different zones of the speleothem substrate (Forti and Perna, 1982). Deposition of the speleothem requires depletion of solute from the surrounding solution, establishing a concentration gradient from the water's surface to the speleothem and thus causing diffusion of nutrient solute toward the growth surface. Fig. 15 shows a scheme wherein a depleted zone forms around growing subaqueous coralloids, with diffu sion flux vectors of new nutrients perpendicular to the iso depleted sur faces. As a consequence, the nutrient amount per unit surface area is greater on the prominences than in the recesses of the substrate. Thus a faster growth rate of subaqueous coralloids on the tips can result from simple diffusion of the solute toward the substrate in the water bulk in subaqueous conditions. This mechanism indicates that coralloid accretion in a subaqueous environment requires the presence of still water near the speleothem. This is because, only if the water is still, there will be a gradient of nutrient depletion to favor faster growth on the prominences of the speleothem (Fig. 15). This also suggests that the growth of smoothing accretions in subaqueous conditions (e.g., formation of subaqueous crusts or mammillary deposits) would re quire a flowing and homogeneous bulk of surrounding solution.

5.6. Isotopic distinction between subaqueous coralloids and subaerial speleothems

Values of $\delta^{13}C$ and $\delta^{18}O$ of subaqueous coralloids are very different from those of subaerial ones. Most strikingly, values of $\delta^{13}C$ and $\delta^{18}O$ of subaqueous coralloids are 12 to 15‰ and 4 to 5‰ less, respectively, than those of subaerial coralloids. This difference provides an important criterion to distinguish these two kinds of coralloids in ancient speleothems. Specifically, it can be useful in understanding the
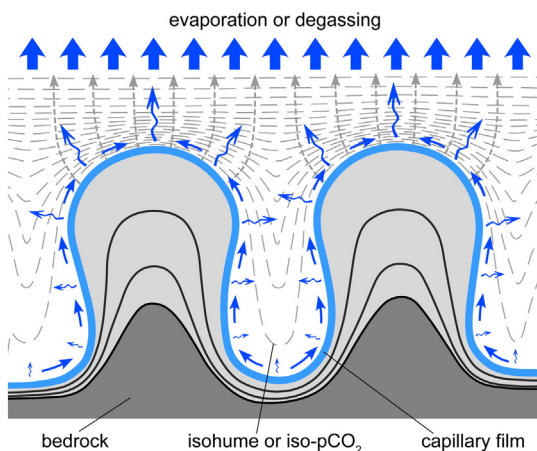

Fig. 13. Sketch showing a model for the growth of subaerial coralloids compatible with the isotopic data obtained in this study and with some genetic hypotheses formulated in the literature. The iso-humidity (or iso-pCO$_2$) curves are less widely spaced near the tips so there the gradient of evaporation is steeper than from depressed zones of the coralloids growth surface. Note that the rate of water loss from protruding regions in a unit of time is much greater than that lost from a more extensive surface of the more depressed zones. Faster evaporation on the tips can explain the movement of the capillary film toward the tips. In addition, the difference in evaporation and CO$_2$ loss between the protrusions and the depressions can also explain the thickness variation in a coralloid accretion.
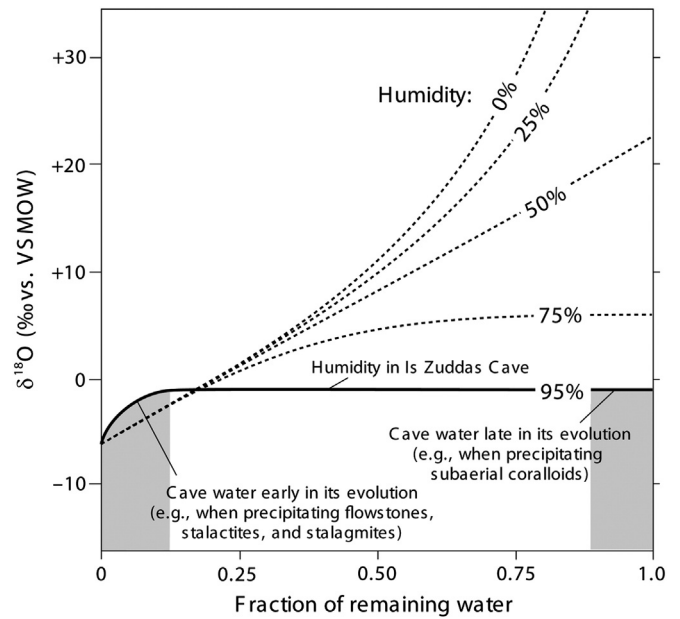

Fig. 14. Oxygen isotope composition of residual water (vertical axis) as a function of the fraction of residual water during evaporation (horizontal axis) and humidity of air into which water evaporates (four dashed curves, and one solid line to emphasize its greatest applicability to spelean conditions). Diagram has been modified from Gat and Gonfiantini (1981).

paleoclimatic significance of stalagmites in which coralloids are present (e.g., Fig. B 11 of Railsback, 2000).

6. Conclusions

This study examines the relationship between the substrate morphol ogy and the isotopic composition ($\delta^{13}C$ and $\delta^{18}O$) of coeval CaCO$_3$ deposits along typical growth layers of massive and coralloid speleothems (smoothing and coralloid accretions). The results lead to several conclusions:

1) Stable isotope data suggest that transport of dissolved solids to subaer ial speleothems can be usefully understood by a model involving input of water in a continuum from gravity to intermediate to capillary stages. Stages nearer to the gravity end of this continuum favor the
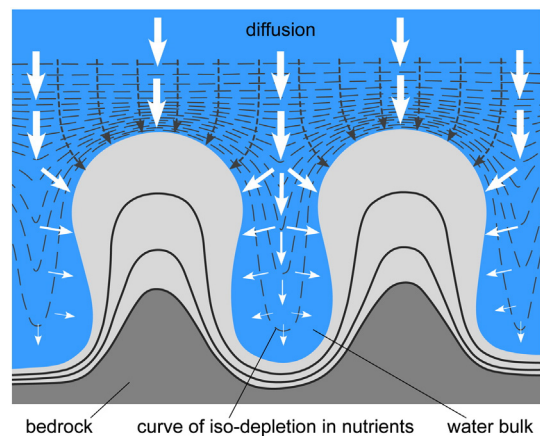

Fig. 15. Sketch showing a model for the growth of subaqueous coralloids compatible with the isotopic data obtained in this study. The curves of iso-depletion in nutrients of the solution are less widely spaced near the tips, so there the mass transfer by diffusion from the water bulk is faster than toward the depressed zones of the growth surface. Note that the net rate of nutrient flow to protruding regions in the unit of time is much greater than that feeding a more extensive surface of the more depressed zones.

growth of massive speleothems, whereas stages nearer to the capillary end favor the growth of coralloids. Thus this study supports the hypothesis that subaerial coralloids form by deposition from predominantly capillary waters, which leads to a greater depositional rate on the prominences. The fluctuation between capillary and gravity stages or various intermediate stages through time may explain how coral loids develop on the surface of previously massive speleothems.

2) Stable isotope data and petrographic observations from subaerial coralloids disprove previous hypotheses that subaerial coralloids form by deposition of solid particles from the air, as an aerosol.

3) Stable isotope data and variation in thickness of laminae suggest that subaqueous coralloids form in static, rather than flowing, pools of water.

4) Stable isotope data readily distinguish between subaerial and subaqueous coralloids, a critical distinction for paleoclimate study of speleothems in which coralloids are present.

5) In subaerial speleothems a greater evaporation rate from protrusions induces capillary water to move toward those areas. This is corroborated especially along smoothing accretions by the pattern of $\delta^{18}O$, whose large variation is made possible by evaporation from water that has previously undergone little evaporation. On the other hand, the relatively small variation in $\delta^{18}O$ along coralloid accretions results from evaporation from water that has previously undergone extensive evaporation, according to the model of Gat and Gonfiantini (1981).

6) In subaerial coralloids, variation in thickness along accretions and a corresponding large variation in $\delta^{13}C$ demonstrate that the coralloid morphology exerts a self reinforcing influence on growth by isolating in its recesses air that is slightly enriched in CO_2 and water vapor compared to the general cave atmosphere, in agreement with the model of Slyotov (1985).

Acknowledgments

References

Alonso-Zarza, A.M., Martín-Pérez, A., Martín-García, R., Gil-Peña, I., Meléndez, A., Martínez-Flores, E., Hellstrom, J., Muñoz-Barco, P., 2011. Structural and host rock controls on the distribution, morphology and mineralogy of speleothems in the Castañar Cave (Spain). Geological Magazine 148 (2), 211–225.

Appelo, C.A.J., Postma, D., 1993. Geochemistry, Groundwater and Pollution. AA Balkema, Rotterdam (536 p.).

Badino, G., Calaforra, J.M., Forti, P., Garofalo, P., Sanna, L., 2011. The present day genesis and evolution of cave minerals inside the Ojo de la Reina Cave (Naica Mine, Mexico). International Journal of Speleology 40 (2), 125–131.

Baker, A., Ito, E., Smart, P.L., McEwan, R.F., 1997. Elevated and variable values of C^{13} in speleothems in a British cave system. Chemical Geology 136 (3–4), 263–270.

Balch, H.E., 1948. Mendip — Its Swallet Caves and Rock Shelters. Clare, Son and Co Ltd., Wells.

Bechstadt, T., Boni, M., 1996. Sedimentological, stratigraphical and ore deposits field guide of the autochthonous Cambro-Ordovician of Southwestern Sardinia. Memorie descrittive della Carta Geologica d'Italia 48, 1–390.

Cabrol, P., 1978. Contribution à l'étude du concrétionnement carbonate des grottes du Sud de la France, morphologie, génèse, diagénèse. Mémoires du Centre d'études et de recherches géologiques et hydrogéologiques 12, 1–275.

Caddeo, G.A., 2011. Studio morfologico e mineralogico-geochimico di speleotemi in cavità carsiche della Sardegna sud occidentale. (PhD Thesis), University of Cagliari, Italia (267 p.).

Caddeo, G., Caredda, A.M., De Waele, J., Frau, F., 2008a. Il ricco patrimonio speleotemico della Grotta di Is Zuddas (Santadi, Sardegna sud-occidentale). Atti del XX Congresso Nazionale di Speleologia, 27–30 Aprile 2007, Iglesias (Italia). Memorie dell'Istituto Italiano di Speleologia II 24, pp. 296–307.

Caddeo, G., De Waele, J., Frau, F., 2008b. Morfologia e meccanismi di crescita per alcune eccentriche aragonitiche della grotta di Is Zuddas a Santadi (Sardegna, Italia). Riassunti del 84° Congresso Nazionale Società Geologica Italiana, 15–17 Settembre 2008, Sassari (Italia). Rendiconti Online Soc. Geol. It. 3, pp. 148–149.

Clark, I.D., Fritz, P., 1997. Environmental Isotopes in Hydrogeology. CRC Press, New York.

Cser, F., Maucha, G., 1968. Contribution to the origin of "excentric" concretions. Karszt-es Barlangkutatas 5 (6), 83–100.

Dawkins, W.B., 1874. Cave Hunting Researches on the Evidence of Caves Respecting the Early Inhabitants of Europe. Macmillan and Co, London (455 p.).

Dreybrodt, W., 1980. Deposition of calcite from thin films of natural calcareous solutions and the growth of speleothems. Chemical Geology 29, 89–105.

Dreybrodt, W., 1981. The kinetics of calcite precipitation from thin films of calcareous solutions and the growth of speleothems: revisited. Chemical Geology 32, 237–245.

Dreybrodt, W., 2008. Evolution of the isotopic composition of carbon and oxygen in a calcite precipitating $H_2O–CO_2–CaCO_3$ solution and the related isotopic composition of calcite in stalagmites. Geochimica et Cosmochimica Acta 72, 4712–4724.

Dublyansky, Y.V., Pashenko, S.E., 1997. Cave Popcorn — An Aerosol Speleothems? Proceedings of the 12th International Congress of Speleology. vol.1. La Chaux-de-Fonds, pp. 271–274

Fairchild, I.J., Baker, A., 2012. Speleothem Science. Wiley-Blackwell, Chichester (432 p.).

Forti, P., Perna, G., 1982. Orientazione dei cristalli di calcite nelle crevasse della miniera di Nebida (Sardegna Sud-occidentale). Periodico di Mineralogia 51, 155–160.

Frisia, S., Borsato, A., Fairchild, I.J., McDermott, F., Selmo, E.M., 2002. Aragonite–calcite relationships in speleothems (Grotte de Clamouse, France): environment, fabrics, and carbonate geochemistry. Journal of Sedimentary Research 72, 687–699.

Gat, J.R., Gonfiantini, R. (Eds.), 1981. Stable Isotope Hydrology: Deuterium and Oxygen-18 in the Water Cycle. IAEA Technical Report Series #210 (Vienna, 337 p.).

Gonzalez, L.A., Lohmann, K.C., 1988. Controls on mineralogy and composition of spelean carbonates, Carlsbad Caverns, New Mexico. In: James, N.P., Choquette, P.W. (Eds.), Paleokarst. Springer-Verlag, New York, pp. 81–101.

Grigor'ev, D.P., 1961. Ontogeny of minerals. Lvov, Izdatel'stvo L'vovskogo Univ. Russian. English Translation 1965. Israel Program for Scientific Translations (250 p.).

Hill, C., Forti, P., 1997. Cave Minerals of the World. National Speleological Society, Huntsville, AL (463 p.).

Istvan, D., Micle, R., 1994. Calcite speleothems generated by underground evapocondensation (Pestera Cobasel, Rodna Mountains). Theoretical and Applied Karstology 7, 183–187.

Klimchouk, A.B., Nasedkin, V.M., Cunningham, K.I., 1995. Cave speleothems of aerosol origin. National Speleological Society Bulletin 57 (1), 31–42 (and 59(1), 45–47).

Maltsev, V.A., 1993. Minerals of the Cupp Coutunn Karst Cave System, Southeast Turkmenistan. vol. 1. World of Stones, Moscow, pp. 5–30.

Maltsev, V.A., 1994. Aerosol Origin of Speleothems: A Critical View of Current Hypothesis. Vopr. Phys. Speleolog. vol. 1, pp. 89–99 (Moscow, In Russian)

Maltsev, V.A., 1997. Stalactites, Crystlactites, Corlactites, Tuflactites — 4 Types of Stalactite-like Formations, Generated from Crystallization Environments With Different Physical Properties. Proceedings of the 12th International Congress of Speleology. vol. 1. La Chaux-de-Fonds, pp. 267–270.

McCrea, J.M., 1950. The isotopic chemistry of carbonates and paleotemperature scale. Journal of Chemical Physics 18, 849.

Moroshkin, V.V., 1976. On the Genesis of Layers of Cristallictite Type. New Data on Minerals of the USSR. 25. Nauka, Moscow.

Onac, B.P., Kearns, J., 2000. Crystallography and mineralogy of multi-aggregates speleothems from Peretele Dârninii Cave (Bihor Mountains, Romania). In: Onac, B.P., Tămaş, T. (Eds.), Proceed. Int. Conf. Karst Studies and Problems. Ed. Presa Universitară Clujeană, Cluj, pp. 87–91.

Perna, G., 1989. Genesi delle concrezioni coralloidi e dei cristalli. Speleologia 20, 40–45.

Railsback, L.B., 2000. An atlas of speleothem microfabrics. http://www.gly.uga.edu/speleoatlas/SAIndex1.html.

Railsback, L.B., Fleisher, C.J., Brook, G.A., Jian, C., Kalin, R., 1994. Environmental controls on the petrology of a late Holocene speleothem from Botswana with annual layers of aragonite and calcite. Journal of Sedimentary Research 64, 147–155.

Self, C.A., Hill, C.A., 2003. How speleothems grow: an introduction to the ontogeny of cave minerals. Journal of Cave and Karst Studies 65 (2), 130–151.

Serban, M., Viehmann, M. I., Coman, D., 1961. Caves of Romania. Ed. Meridiane, Bucharest.

Slyotov, V.A., 1985. Concerning the ontogeny of crystallictite and helictite layers of calcite and aragonite from the karst caves of southern Fergana. Novye Dannye o Mineralakh CCCP (new data on minerals), Nauka, Moscow, vol. 32, 119–127. In Russian. English translation 1999. Cave Geology 2 (4), 196–208.

Stepanov, V.I., 1997. Notes on mineral growth from the archive of V. I. Stepanov (1924–1988). Proceedings of the University of Bristol Spelaeological Society 21 (1), 25–42.

Stepanov, V.I., 1999. Periodicity of crystallization processes in karst caves. Cave Geology 2, 209–220 (English translation of Russian paper appeared in 1971).

Thrailkill, J.V., 1965. Origin of cave popcorn. National Speleological Society Bulletin 27 (2), 59.

White, W.B., 2012. Speleothem microstructure/speleothem ontogeny: a review of Western contributions. International Journal of Speleology 41 (2), 329–358.